Electronic Supplementary Material (ESI) for New Journal of Chemistry.

Supporting Information

Synthesis and properties of hollow Fe_3O_4@Au hybrid nano-structures for T_1-T_2 MR imaging and combination of magnetic and photo-induced heating

Nguyen T. N. Linh[a], Ngo T. Dung[b]*, Le T. T. Tam[b], Le T. Tam[c], Nguyen P. Hung[a], Nguyen D. Vinh[a], Ngo T. Ha[a], Pham. H. Nam[e], Le V. Thanh[f], Nguyen V. Dong[f], Le G. Nam[f], Nguyen V. Dang[a], Nguyen X. Phuc[e], Le D. Tung[g,h], Nguyen T. K. Thanh[g,h] and Le T. Lu[b,d]*

[a]Thai Nguyen University of Sciences, Tan Thinh Ward, Thai Nguyen City, Thai Nguyen, Vietnam.
[b]Institute for Tropical Technology, Vietnam Academy of Science and Technology (VAST), 18 Hoang Quoc Viet, Hanoi, Vietnam.
[c]Vinh University, 182 Le Duan Street, Vinh City, Nghe An, Vietnam.
[d]Graduate University of Science and Technology, VAST, 18 Hoang Quoc Viet, Hanoi, Vietnam.
[e]Institute of Materials Science, VAST, 18 Hoang Quoc Viet, Hanoi, Vietnam.
[f]Vinh International Hospital, 99 Pham Dinh Toai Street, Vinh City, Nghe An, Vietnam
[g]Biophysics Group, Department of Physics and Astronomy, University College London, Gower Street, London WC1E 6BT, U
[h]UCL Healthcare Biomagnetics and Nanomaterials Laboratories, University College London, 21 Albemarle Street, London W1S 4BS, UK.

Table S1. Influence of synthesis conditions on the Fe_3O_4 particle size.

$Fe(acac)_3$ (mM)	OA (mM)	OLA (mM)	OCD-ol (mM)	T (°C)	T (min)	Size (nm)
190	744	744	300	295	10	3.4 ± 0.5
					30	6.7 ± 0.7
					60	8.1 ± 0.7
					120	13.9 ± 1.1
190	558	558	300	295	60	6.3 ± 0.9
	744	744				8.1 ± 0.7
	930	930				14.7 ± 1.3
190	744	744	300	295	30	6.7 ± 0.7
673						7.2 ± 0.9
920						14.3 ± 1.5

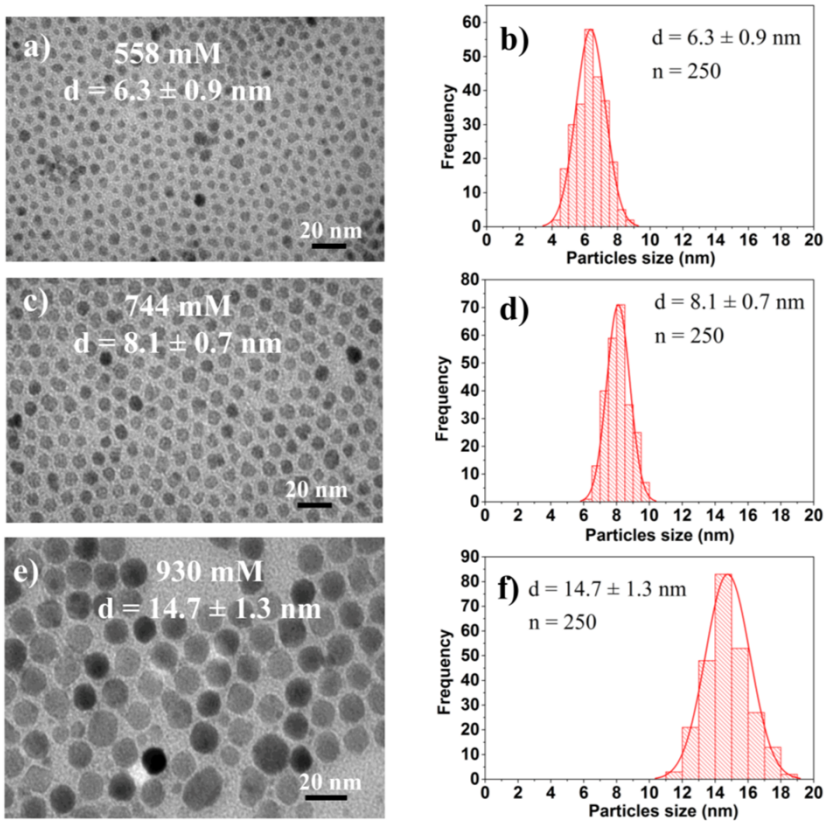

Fig. S1 TEM images and their corresponding size distribution histograms of Fe_3O_4 nanoparticles synthesised with different surfactant concentrations: 558 mM (a, b), 744 mM (c, d), 930 mM (e, f).

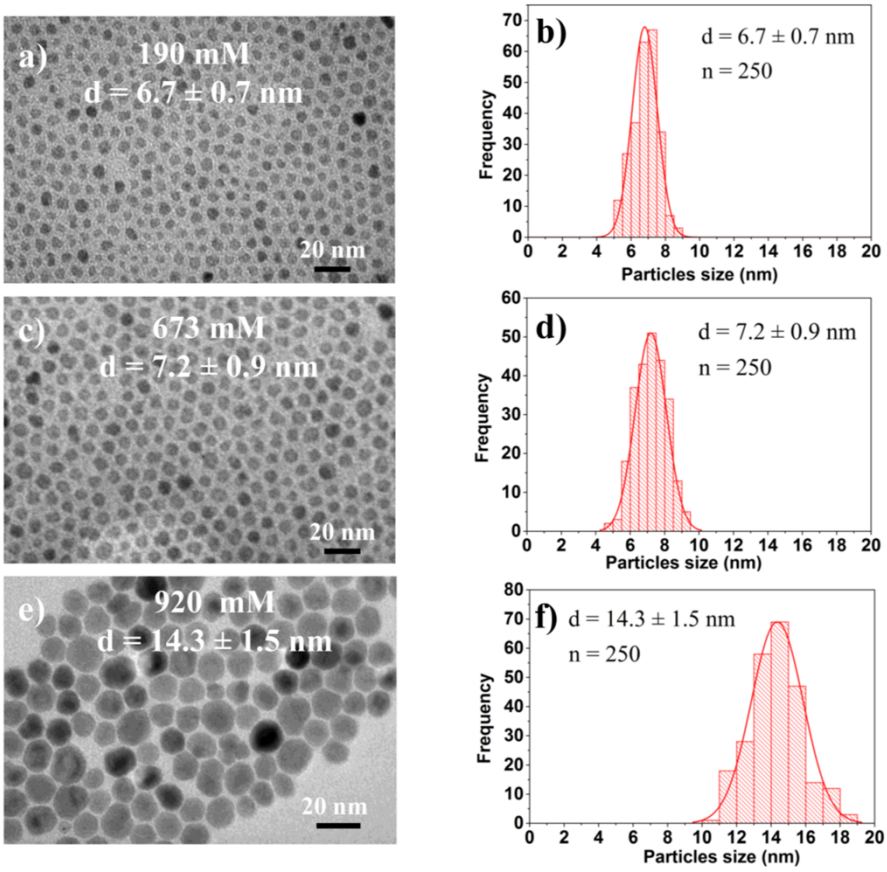

Fig. S2 TEM images and their corresponding size distribution histograms of Fe_3O_4 nanoparticles synthesised with different precursor concentrations: 190 mM (a, b), 673 mM (c, d), 920 mM (e, f).

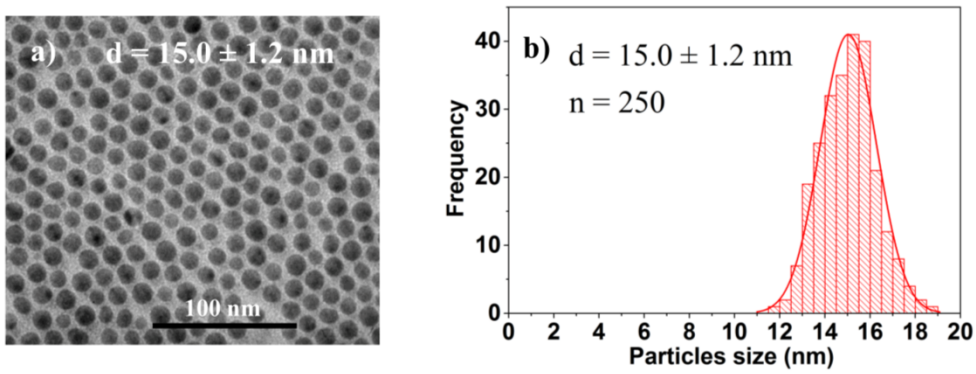

Fig. S3 TEM image and size distribution histogram of Ag nanoparticles synthesised under similar conditions but without Fe_3O_4 NPs at reaction time of 60 min.

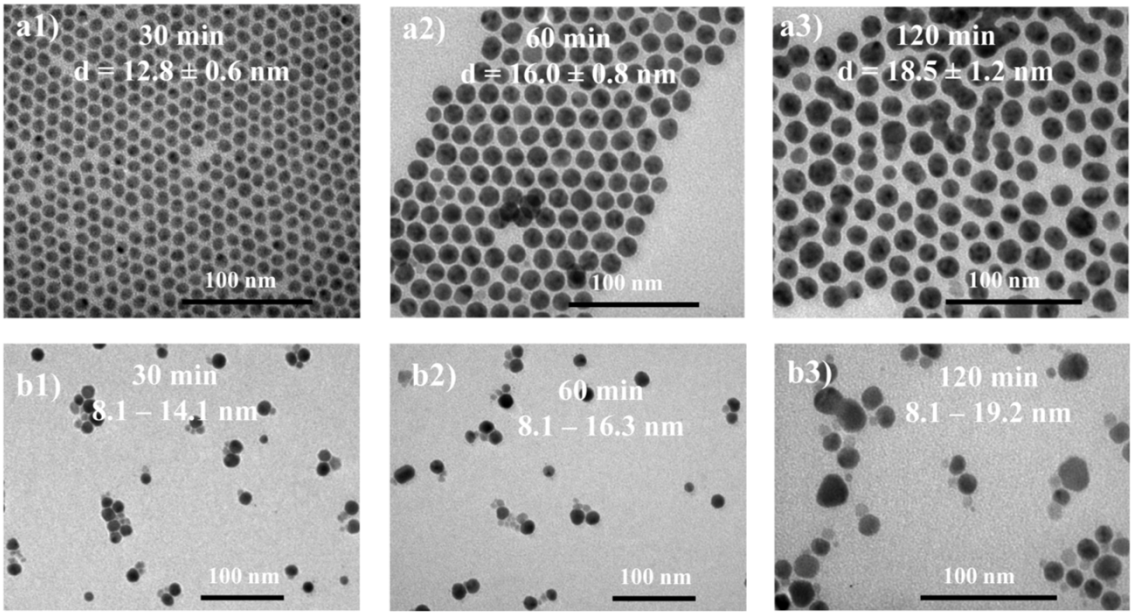

Fig. S4 TEM images of HNPs synthesised with Fe_3O_4 seeds of 8.1 nm at different reaction times: (a1-a3) core-shell Fe_3O_4@Ag HNPs and (b1-b3) dumbbell-like Fe_3O_4-Ag HNPs.

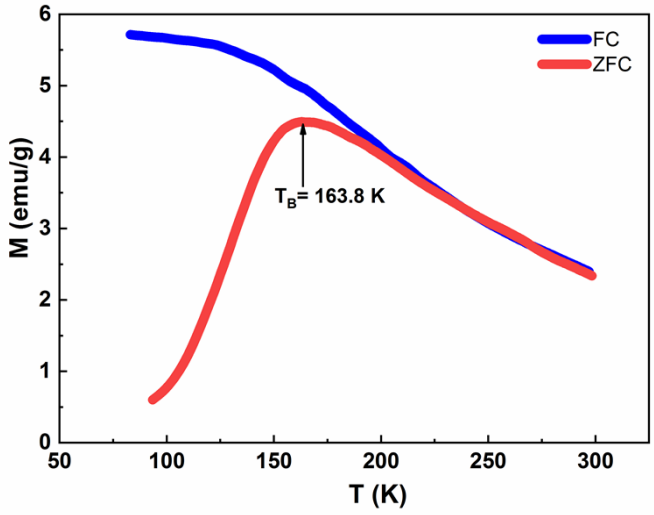

Fig. S5 Temperature dependence of magnetization (in ZFC and FC regimes at a magnetic field of 8 kA/m) for Fe_3O_4 NPs (8.1 ± 0.7 nm).

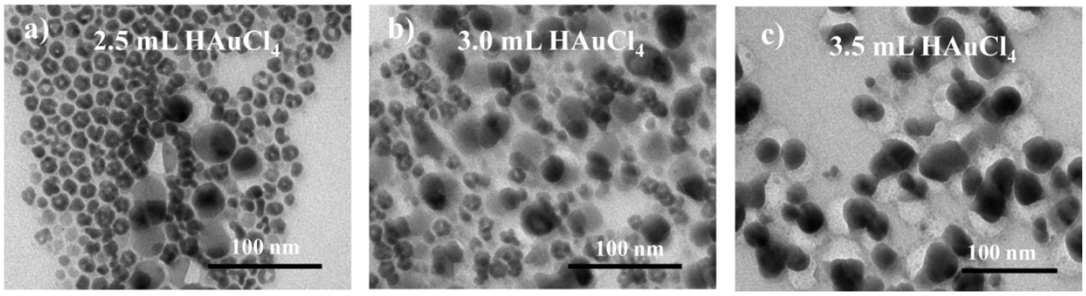

Fig. S6 TEM images of Fe_3O_4@Au h-NPs prepared at different $HAuCl_4$ solution volumes: 2.5 (a), 3.0 (b) and 3.5 mL (c) showing the formation of solid NPs.

Table S2. Effect of the amount of $HAuCl_4$ solution on the size and morphology of h-NPs.

The volumes of $HAuCl_4$ solution (mL)	The particle size (nm)	Morphology
0	16.0 ± 0.8	Solid sphere (Fe_3O_4@Ag templates)
0.5	16.1 ± 0.8	Solid sphere
1.0	16.4 ± 0.9	Hollow sphere
1.5	16.6 ± 1.0	Hollow sphere
2.0	17.0 ± 1.1	Hollow sphere
2.5	18.8 ± 2.1	Hollow sphere and solid sphere
3.0	26.3 ± 3.4	Hollow sphere and solid sphere
3.5	33.2 ± 5.7	Solid sphere

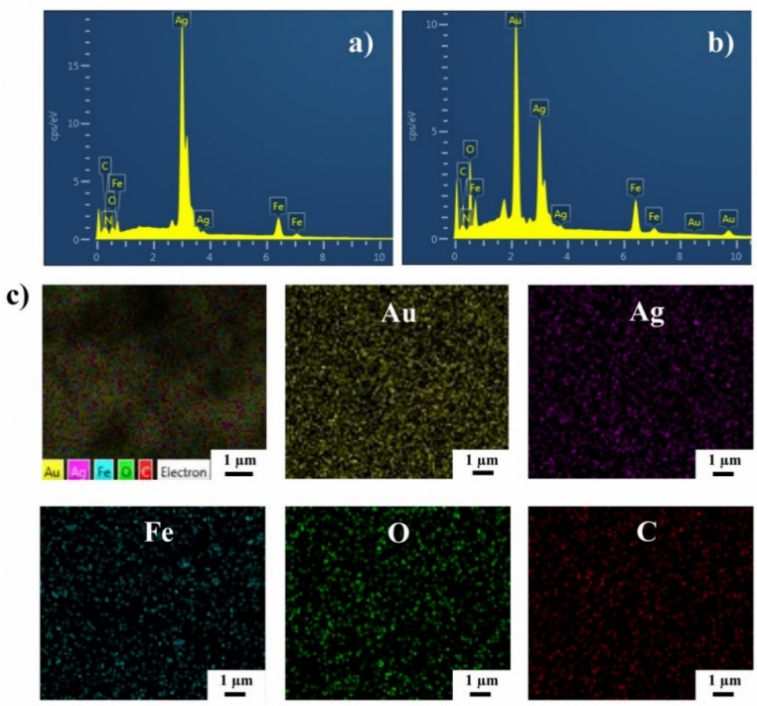

Fig. S7. EDS spectra of Fe_3O_4@Ag nanotemplates (a) and hollow Fe_3O_4@Au h-NPs (b); and EDS elemental mapping of hollow Fe_3O_4@Au h-NPs (c) prepared at 2.0 mL $HAuCl_4$ solution.

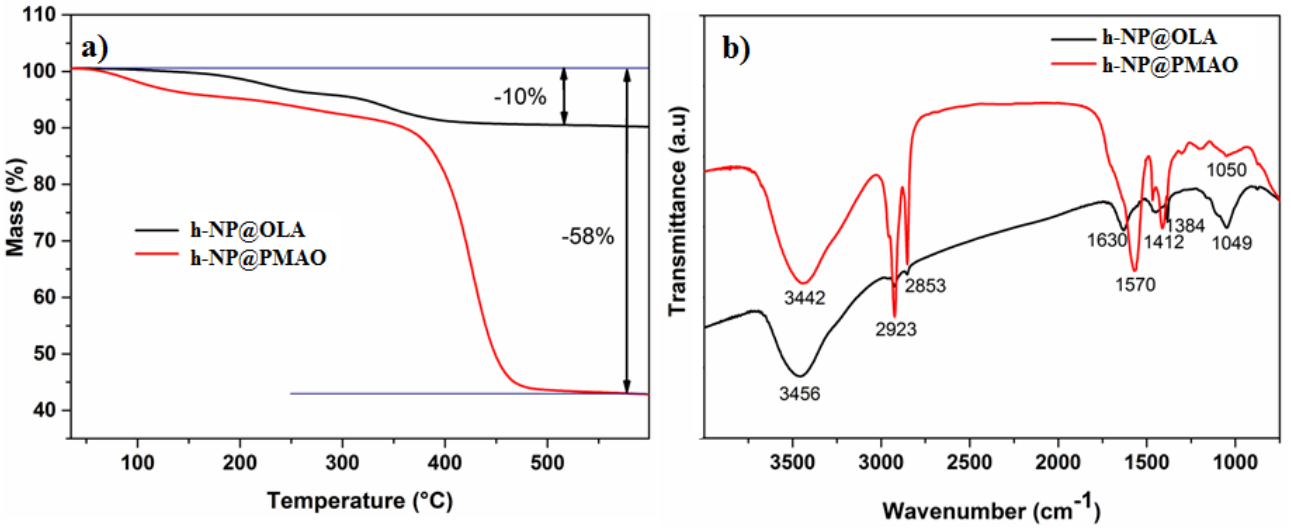

Fig. S8. a) TGA scans and b) FT-IR spectra of OLA and PMAO encapsulated hollow Fe_3O_4@Au h-NPs.

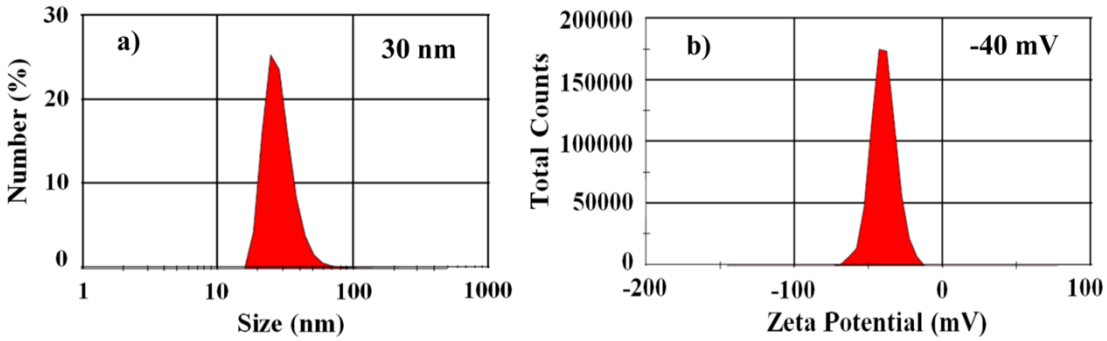

Fig. S9 Hydrodynamic size distribution (a) and zeta potential (b) of PMAO encapsulated hollow Fe_3O_4@Au HNPs.

Table S3. MRI relaxivities of the commercial gadolinium-(GBCAs), iron oxide nanoparticle-based contrast agents and the hollow Fe_3O_4@Au h-NPs.

Brand Name	Ligand shell/Generic Name (INN)	Core size (nm)	Overall size (nm)	r_1 (mM^{-1} s^{-1})	r_2 (mM^{-1} s^{-1})	r_2/r_1	Company/refs
Hollow Fe_3O_4@Au h-NPs	**PMAO**	**17.0**	**28.84**	**8.47**	**74.45**	**8.79**	**Current study**
Dotarem®	Gadoterate meglumine (Gd-DOTA)	-	-	3.6 (3.4-3.8)	4.3 (3.4-5.2)	1.19	Belgium for Guerbet[1]
Magnevist®	Gadopentetate dimeglumine (Gd-DTPA)	-	-	4.1 (3.9–4.3)	4.6 (3.8–5.4)	1.12	Bayer Schering (Germany)[1]
MultiHance®	Gadobenate dimeglumine (Gd-BOPTA)	-	-	6.3 (6.0–6.6)	8.7 (7.8–9.6)	1.38	Bracco[1]
Omniscan®	Gadodiamide (Gd-DTPA BMA)	-	-	4.3 (4.0–4.6)	5.2 (4.2–6.2)	1.21	GE Healthcare[1]
ProHance®	Gadoteridol (Gd-HPDO3A)	-	-	4.1 (3.9–4.3)	5.0 (4.2–5.8)	1.22	Bracco[1]

Gadovist®	Gadobutrol (Gd-DO3A-butrol)	-	-	5.2 (4.9–5.5)	6.1 (5.2–7.0)	1.17	Bayer Schering (Germany)[1]
Teslascan®	Mangafodipir trisodium (Mn-DPDP)	-	-	1.6 (1.5–1.7)	2.1 (1.4–2.8)	1.31	Amersham[1]
Ferumoxtran (Sinerem)	Dextran + citrate	4.5	34	5.0	66.0	13.2	[2]
VSOP-C184	Citrate	8.6	19	8.0	34	4.25	[3]
Ferumoxytol®	Dextran (C7228)	6.7	35	7.5	92	12.26	AMAG Pharma-ceutical Inc[4]
Resovist®	Ferucarbotran (SHU 555 A) Carboxydextran		60	7.4	151	20.40	Schering[1]
Feridex/Endorem®	Ferumoxide (AMI-25) Dextran	4.5	160	10.1	120	11.88	Berlex/Guerbet [5]
Ferucarbotran®/ Supravist	Ferucarbotran (SHU555C) Dextran	3-5	21	7.3	57	7.81	Schering[6]
PEG (5) – BP - USPIO	PEG-bisphosphonate[b]	5.5	23	9.5 (3.0 T)	28.2 (3.0 T)	2.97	[3]
ESION	PEG-phosphine oxide (γ-Fe_2O_3)	2.2	15	4.8 (3.0 T)	29.2 (3.0 T)	6.08	[7]
USPIO	PEG-phosphine oxide (Fe_3O_4)	12	-	2.37 (3.0 T)	58.8 (3.0 T)	24.81	[7]
GdIO	Dopaminesulfonate Fe_3O_4+Gd_2O_3	4.8	6.50	7.85 (0.5 T)	41.14 (0.5 T)	5.24	[8]
MnMEIO	2,3-dimercaptosuc-cnic acid (DMSA) $MnFe_2O_4$	12	-	-	358	-	[9]
NiMEIO	2,3-dimercaptosuc-cnic acid (DMSA) $NiFe_2O_4$	-	-	-	152	-	[9]
Au-Fe_3O_4 heterodimer	-	-	30.4	-	245 (3.0T), 723 HU at 100 mM Au	-	[10]
F-AuNC@ Fe_3O_4	Au nanocages Folic acid functionalized	2.2	110	6.26	28.11	4.49	[11]

[b]1,2-distearoyl-sn-glycero-3-phosphoethanolamine-N-[methoxy(polyethylene glycol)-2000].

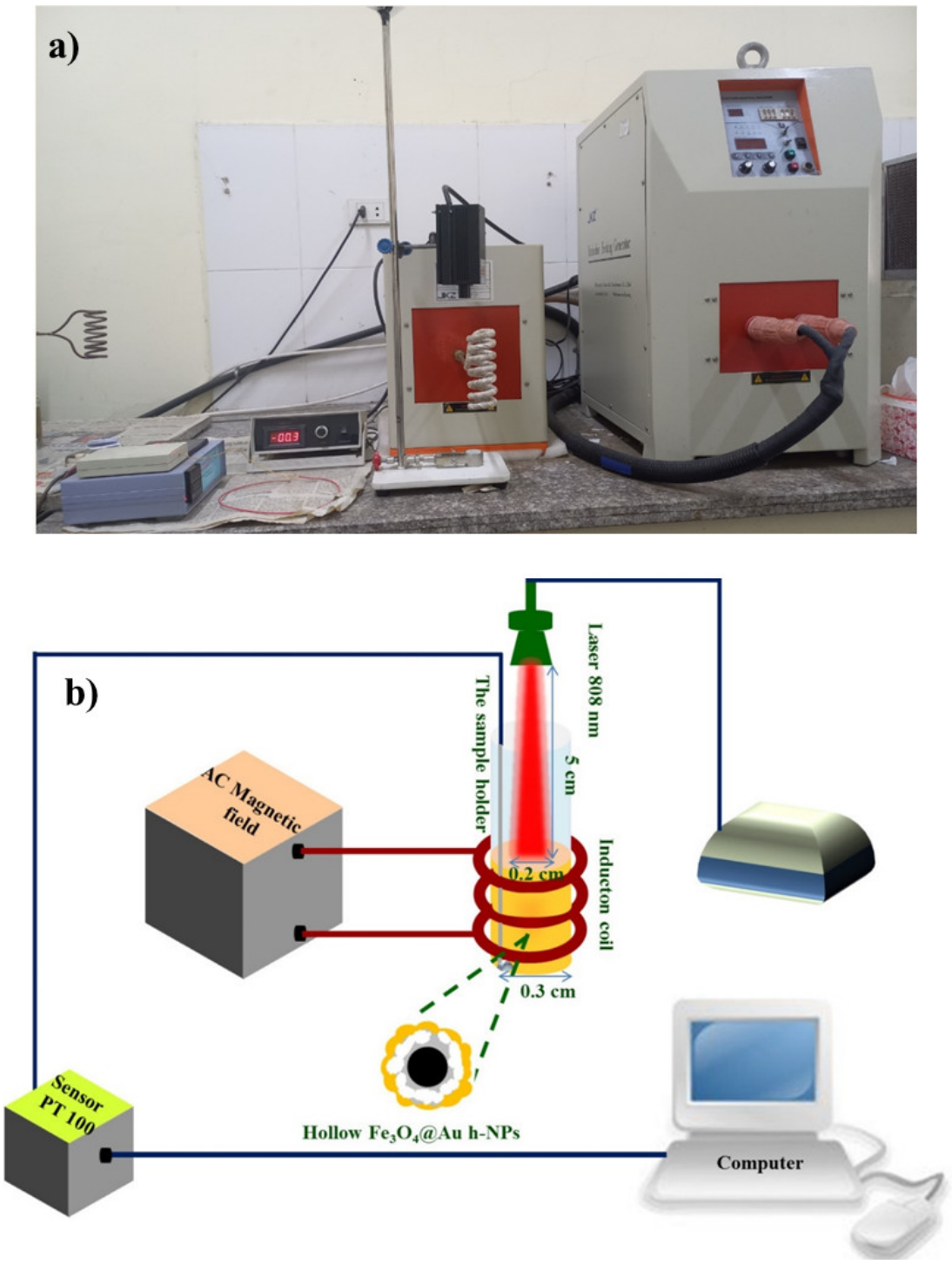

Fig. S10 The magnetic and photoinduced heating experiment (a) and schematic diagram (b)

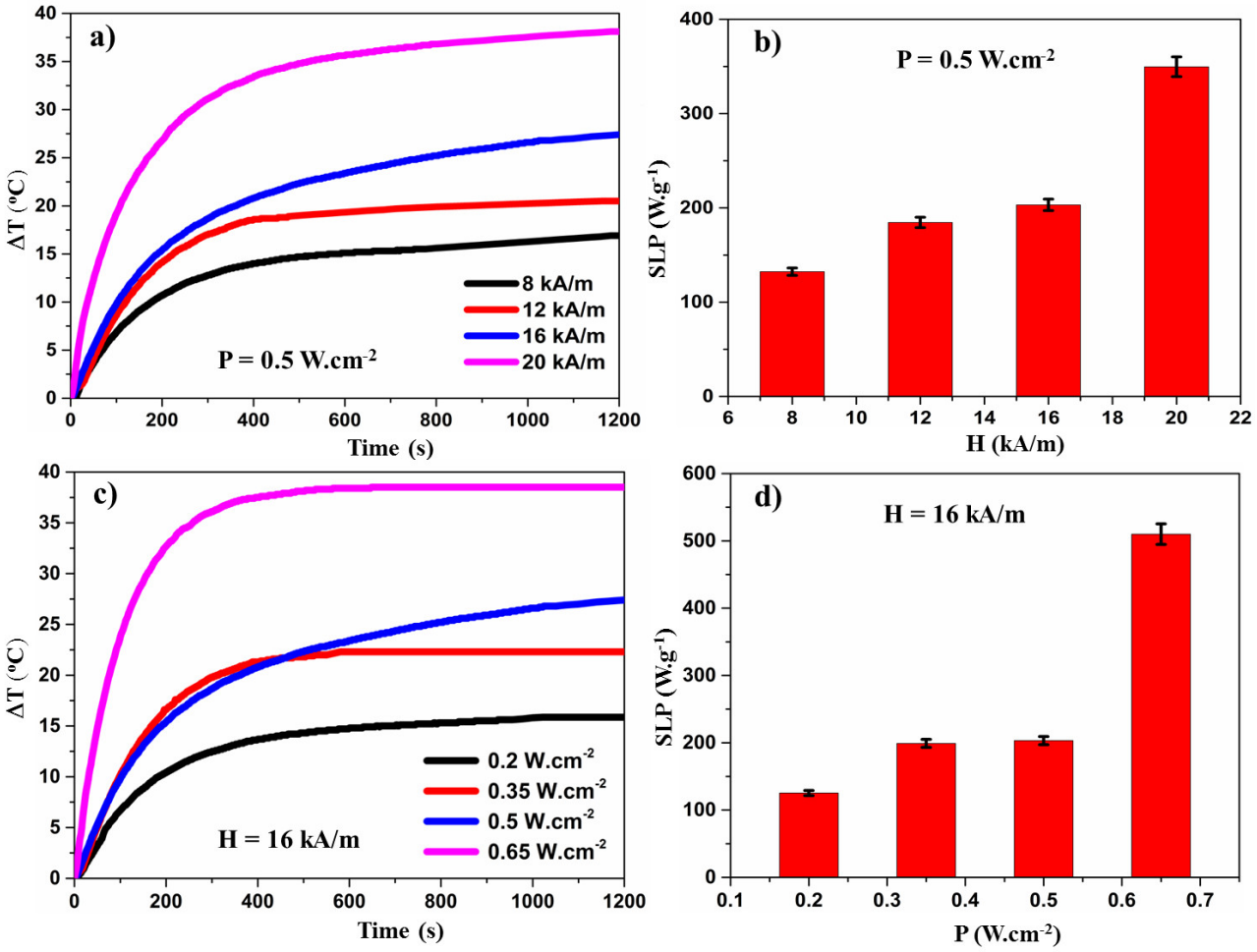

Fig. S11 The heating curves (a), and the corresponding SLP values (b) for the hollow Fe_3O_4@Au h-NPs solutions under different applied fields (from 8 to 20 kA/m) at a constant frequency of 450 kHz and a laser power density 0.5 W.cm^{-2}. The heating curves (c), and the corresponding SLP values (d) for the h-NPs solution under a constant applied field of 16 kA/m at a frequency 450 kHz and different power densities (from 0.2 to 0.65 W.cm^{-2}).

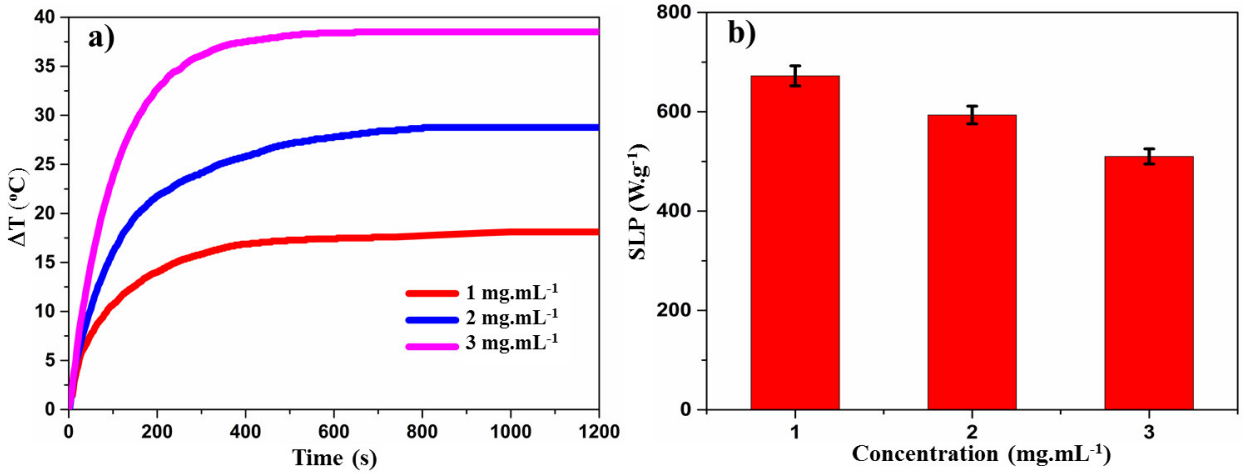

Fig. S12 The heating curves (a), and the corresponding SLP values (b) for the hollow Fe_3O_4@Au h-NPs solutions at different concentrations under an applied field of 16 kA/m at a frequency 450 kHz and a laser power density 0.65 W.cm^{-2}

References

1 M. Rohrer, H. Bauer, J. Mintorovitch, M. Requardt and H.-J. Weinmann, *Invest. Radiol.*, 2005, **40**, 715-724.
2 M. F. Casula, P. Floris, C. Innocenti, A. Lascialfari, M. Marinone, M. Corti, R. A. Sperling, W. J. Parak and C. Sangregorio, *Chem. Mater.*, 2010, **22**, 1739-1748.
3 L. Sandiford, A. Phinikaridou, A. Protti, L. K. Meszaros, X. Cui, Y. Yan, G. Frodsham, P. A. Williamson, N. Gaddum, R. M. Botnar, P. J. Blower, M. A. Green, and R. T. M. de Rosales, *ACS Nano*, 2013, **7**, 500-512.
4 W. Li, S. Tutton, A. T. Vu, L. Pierchala, B. S. Y. Li, J. M. Lewis, P. V. , and R. R. Edelman, *J. Magn. Reson. Imaging*, 2005, **21**, 46-52.
5 D. L. J. Thorek, A. K. Chen, J. Czupryna and A. Tsourkas, *Ann. Biomed. Eng.*, 2006, **34**, 23-38.
6 N. Chan, M. Laprise-Pelletier, P. Chevallier, A. Bianchi, M. A. Fortin, and J. K. Oh, *Biomacromolecules*, 2014, **15**, 2146-2156.
7 B. H. Kim, N. Lee, H. Kim, K. An, Y. Il Park, Y. Choi, K. Shin, Y. Lee, S. G. Kwon, H. B. Na, J.-G. Park, T.-Y. Ahn, Y.-W. Kim, W. K. Moon, S. H. Choi and T. Hyeon, *J. Am. Chem. Soc.*, 2011, **133**, 12624-12631.
8 Z. Zhou, L. Wang, X. Chi, J. Bao, L. Yang, W. Zhao, Z. Chen, X. Wang, X. Chen and J. Gao, *ACS nano*, 2013, **7**, 3287-3296.
9 J. H. Lee, Y. M. Huh, Y. W. Jun, J. W. Seo, J. T. Jang, H. T. Song, S. Kim, E. J. Cho, H. G. Yoon, J. S. Suh and J. Cheon, *Nat. Med.*, 2007, **13**, 95-99.
10 D. Kim, M. K. Yu, T. S. Lee, J. J. Park, Y. Y. Jeong, and S. Jon, *Nanotechnology*, 2011, **22**, 155101-155107.
11 G. Wang, W. Gao, X. Zhang and X. Mei, *Sci. Rep.*, 2016, **6**, 28258-28267.